Quark–hadron duality in inclusive electron–proton scattering at high Q^2: Structure functions and W-truncated moments from CLAS12

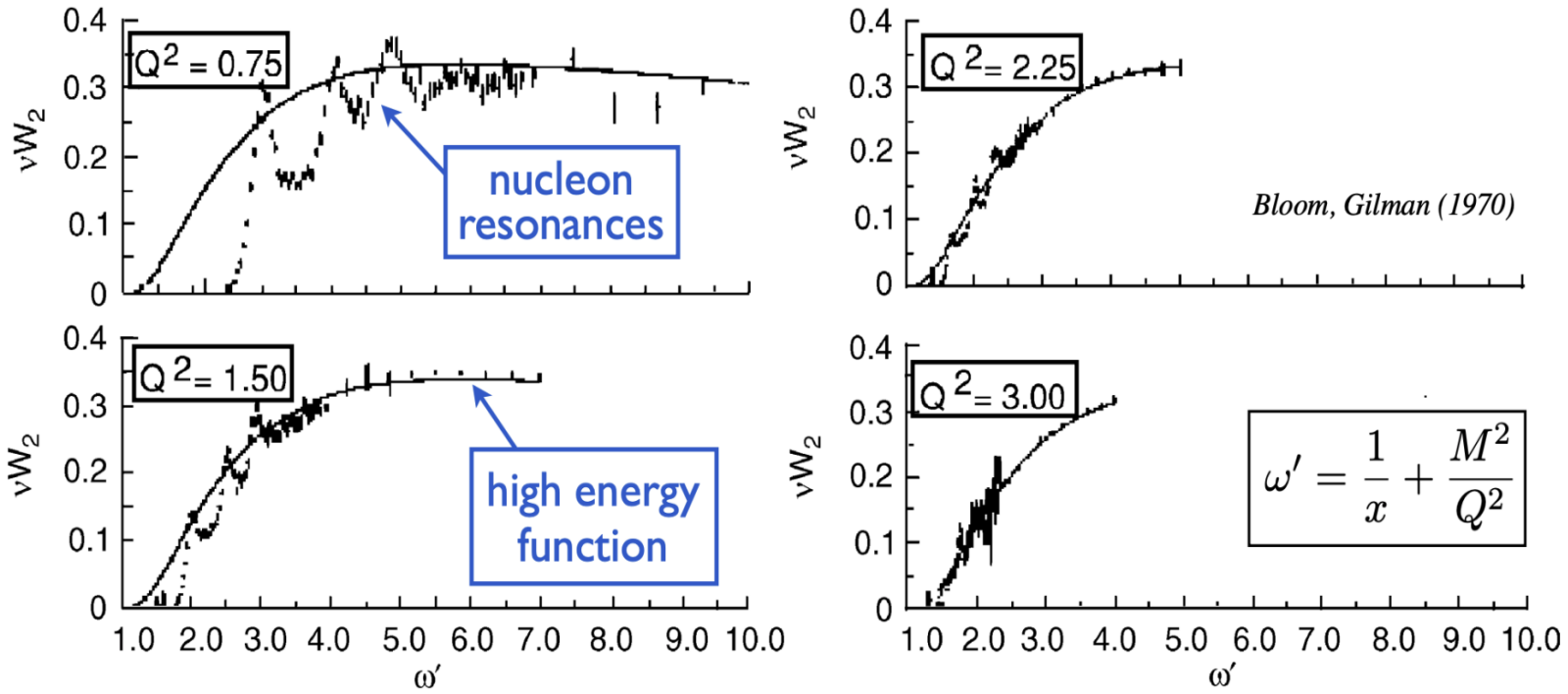
Aleksandr Bulgakov[1], Yannick Wunderlich[1], Kyungseon Joo[1], Viktor Mokeev[2], T.-S. Harry Lee[3]

1 - University of Connecticut 2 - Thomas Jefferson National Accelerator Facility 3 - Argonne National Laboratory

CLAS collaboration meting

18th November 2026

Duality: resonance averages reproduce DIS scaling



Adapted from [Bloom and Gilman (1970, 1971)]

- Local duality: agreement after averaging within individual resonance regions.
- Global duality: agreement only after averaging over the full resonance region.

Hadronic picture

At W $\lesssim$ 2 GeV, inclusive ep scattering shows explicit N* resonance structure.

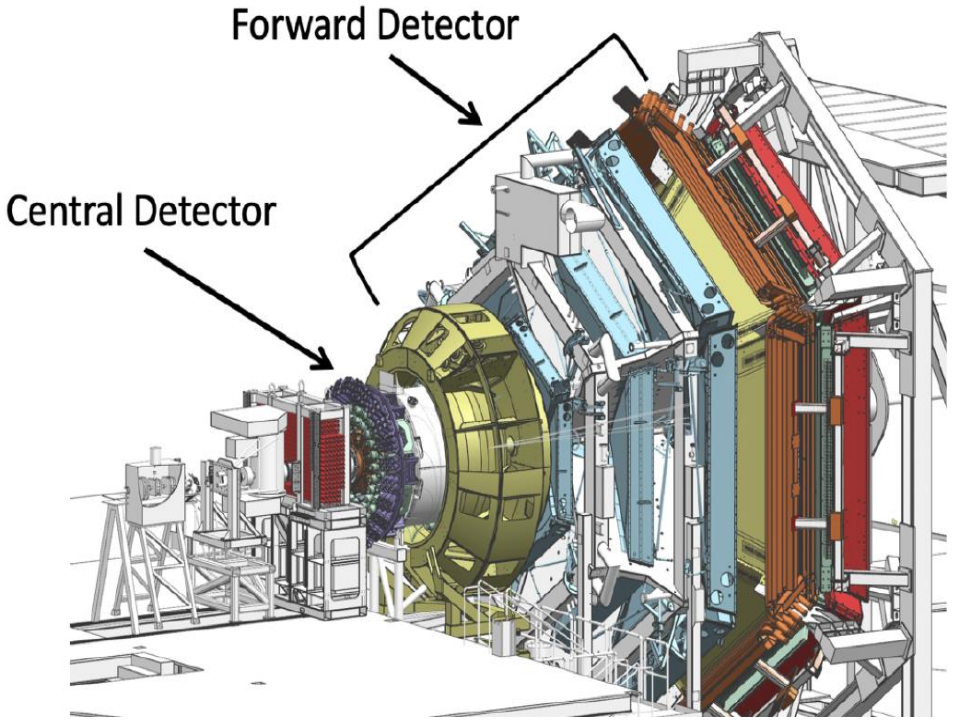
average over W →

Partonic picture

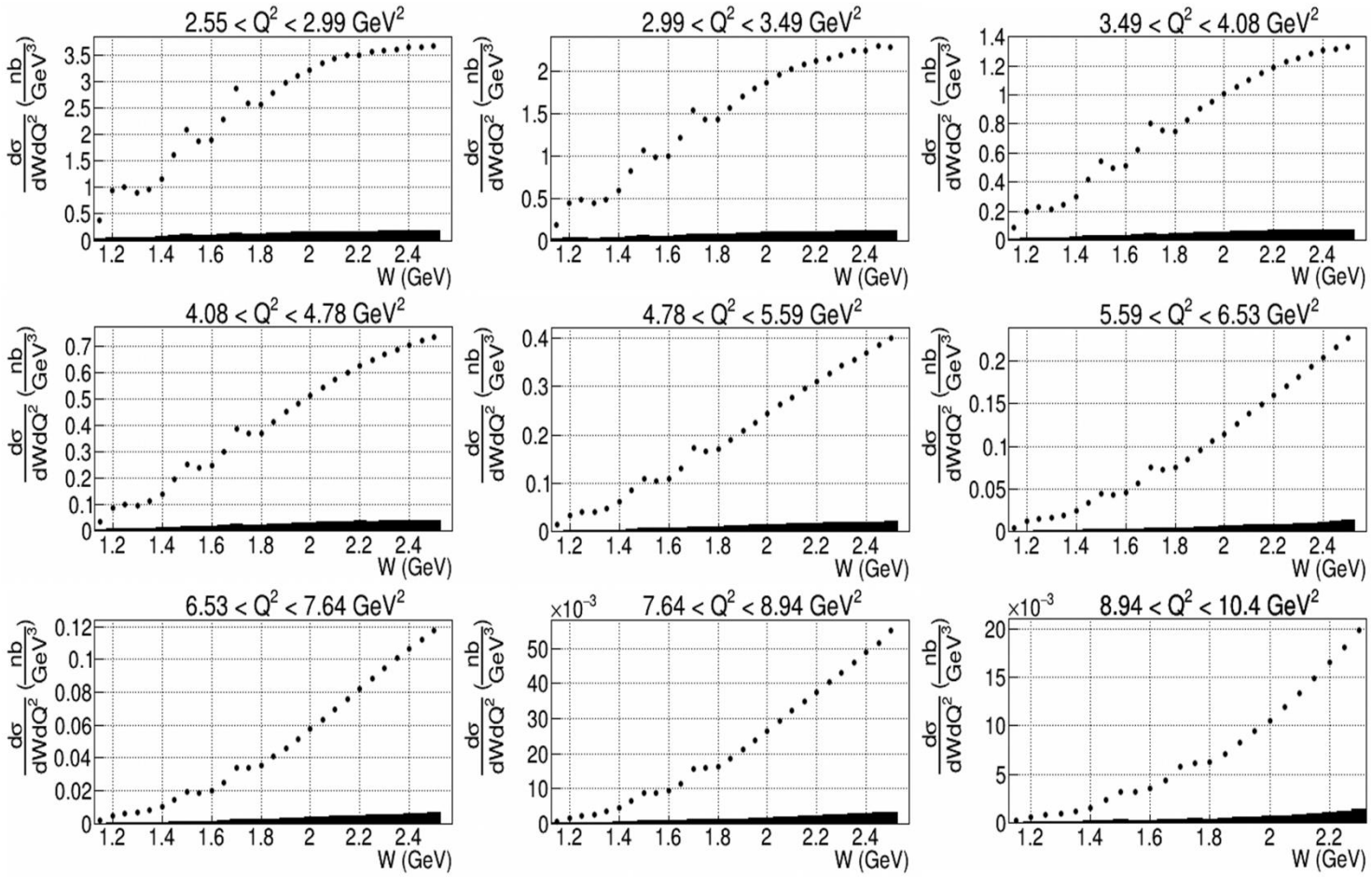
At larger W and Q^2, the same observables are described with PDFs and QCD corrections.

CLAS12 extends resonance-region duality tests to higher Q^2

- Inclusive $e\ p \rightarrow$ e' p' X scattering
- RG-A Fall2018 Pass 1Inbending
- E_{beam} = 10.6 GeV
- Nine Q^2 bins: $2.55 \leq Q^2 \leq 10.4$ GeV^2
- W from pion threshold to about 2.5 GeV



CLAS12 Detector



Inclusive differential cross section $\frac{d^2\sigma}{dW dQ^2}$

V. Klimenko et al. (CLAS Collaboration), Phys. Rev. C 112, 025201 (2025)

Introducing ANL-Osaka model and CJ15 parton distribution functions

HADRONIC

ANL–Osaka model (EBAC @ JLab)

- Dynamical coupled-channels (DCC) model — resonances + non-resonant background.
- Inclusive strength built from πN, ηN, KΛ, KΣ and ππN channels (incl. πΔ, ρN, σN).
- Provides explicit hadronic degrees of freedom with correct thresholds.
- **ANL–Osaka describes the resonance region up to $Q^2 \sim 3\ GeV^2$.**



PARTONIC

CJ15 NLO global QCD analysis

- Using PDFs to construct structure function F_2 and inclusive cross sections
- PDFs are taken from LHAPDF 6.5.4.
- **CJ15NLO + LT — leading-twist baseline.**
- **CJ15NLO + TMC + HT — adds target-mass + higher-twist corrections.**
- The CJ15NLO + TMC + HT curve is the smooth reference duality should reproduce.

Connecting hadronic and partonic descriptions

PDF-based calculations of the F_2 structure function

$$F_2^{\mathrm{LO\,LT}}(x) = 2xF_1(x) = x\sum_q e_q^2\,[q(x)+\bar{q}(x)]$$

$$F_2^{\mathrm{NLO,LT}}(x,Q^2) = x\sum_q e_q^2\left\{[q+\bar{q}]\otimes\left[\delta(1-z)+\frac{\alpha_s(Q^2)}{2\pi}C_{2,q}^{(1)}(z)\right]+\frac{\alpha_s(Q^2)}{2\pi}\,g\otimes C_{2,g}^{(1)}(z)\right\}$$

$$F_2^{\mathrm{OPE}}(x,Q^2) = \frac{(1+\rho)^2}{4\rho^3}F_2^{\mathrm{NLO,LT}}(x_N,Q^2)+\frac{3x(\rho^2-1)}{2\rho^4}\left[A(x_N,Q^2)+\frac{\rho^2-1}{2x\rho}\,B(x_N,Q^2)\right]$$

where $A(x_N,Q^2)=\int_{x_N}^1 du\,\frac{F_2^{\mathrm{NLO,LT}}(u,Q^2)}{u^2}$, $\quad B(x_N,Q^2)=\int_{x_N}^1 du\,(u-x_N)\frac{F_2^{\mathrm{NLO,LT}}(u,Q^2)}{u^2}$

$$F_2^{\mathrm{NLO,HT,TMC}}(x,Q^2) = F_2^{\mathrm{OPE}}(x,Q^2)\left(1+\frac{C_{\mathrm{HT}}(x)}{Q^2}\right)$$

where

$C_{\mathrm{HT}}(x) = h_0 x^{h_1}(1+h_2 x)$, $h_0 = -3.2874 \pm 0.26061, h_1 = +1.9274 \pm 0.10524, h_2 = -2.0701 \pm 0.019888$

Formulae adapted from A. N. Hiller Blin et al., Phys. Rev. C 104, 025201 (2021).

Leading order
Leading twist (LO LT)

↓

Next-to-leading order
Leading twist (NLO LT)

↓

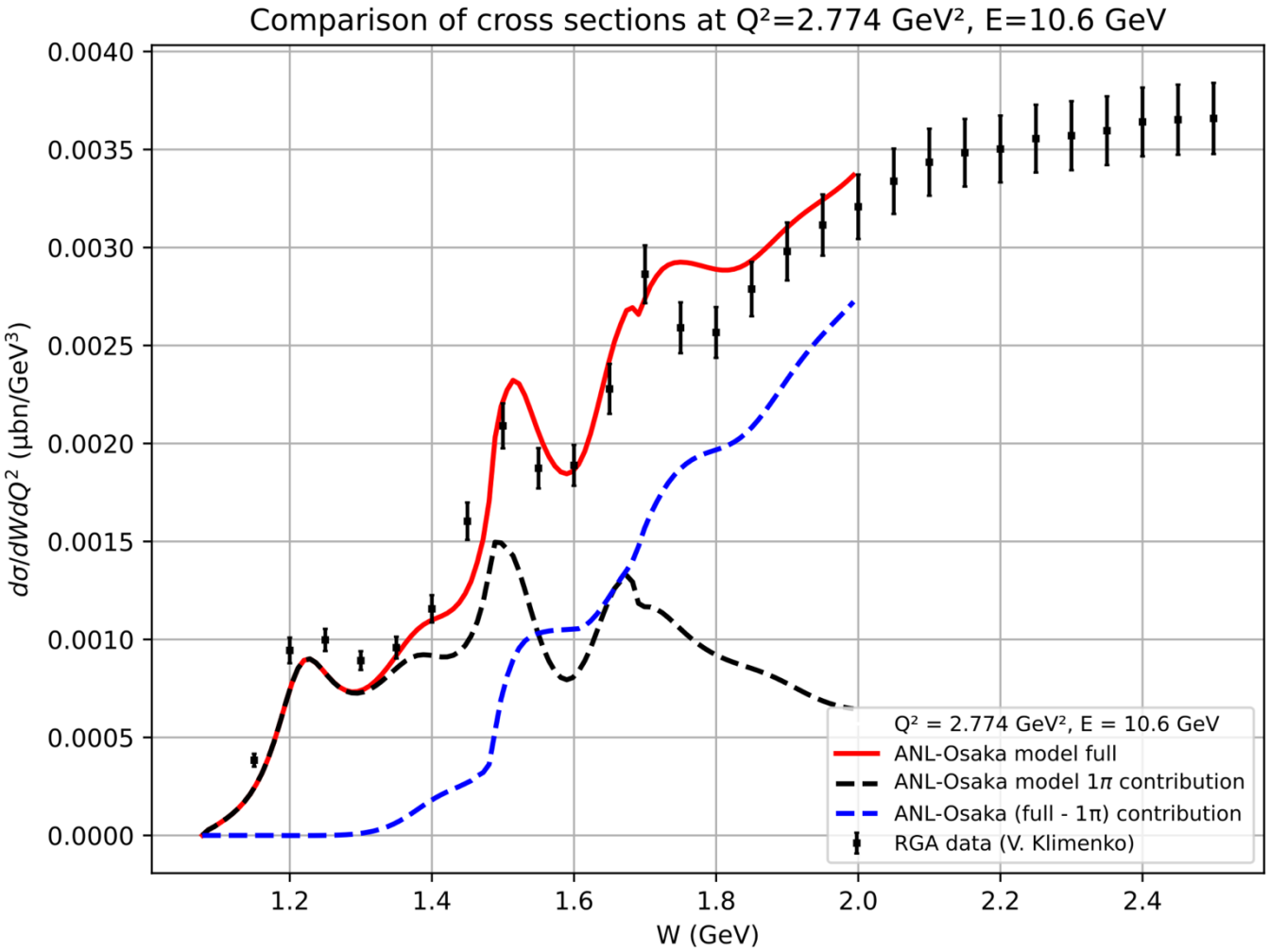
NLO leading twist+ TMC (OPE)

↓

NLO leading twist + HT + TMC (OPE)

TMC = target-mass corrections
OPE = operator product expansion
HT = higher twist

Introducing ANL-Osaka dynamic coupled channel model @ $Q^2 = 2.774\ GeV^2$



- Full AO reproduces the resonance structure at the anchor Q_0^2 = 2.774 GeV^2
- The exclusive 1π channel alone underestimates the inclusive cross section
- Multi-meson channels are essential for reproducing the inclusive resonance region strength and for realizing quark–hadron duality above the 1st resonance region
- The full ANL-Osaka calculation provides the natural hadronic-basis input for the high-Q2 extension

Analysis chain

1 Measured cross section

Experimental input: $\frac{d^2\sigma}{dW dQ^2}$, nine Q^2 bins from 2.55 to 10.4 GeV², covering the entire resonance region.

→

2 Hadronic basis: ANL-Osaka model

Anchor at $Q_0^2 = 2.774$ GeV², where ANL–Osaka describes the data, and extend phenomenologically to higher Q^2.

→

3 Fit 1 — extend

Evolve the 1π and 2π pieces from the anchor to reach higher Q^2 — the Ansatz describes the data to 10 GeV².

→

→

4 Fit 2 — apply

Same Ansatz, now on the L/T axis: σ_T and σ_L evolved separately from the anchor, $R_{LT} = \sigma_L/\sigma_T$ constrained to the ANL–Osaka value with 30% tolerance.

→

5 Structure function

$F_2 = Kv(\sigma_T + \sigma_L) / [4\pi^2\alpha_{em}(1 + v^2/Q^2)]$, evaluated bin by bin.

→

6 Duality test

Truncated moments M_2 over four contiguous W windows, compared with CJ15+LT and CJ15+TMC+HT.

Fit 1 separates 1π and multi-meson strength. “Step 3”

$$\sigma(W,Q^2) = \tilde{\sigma}^{1\pi}(W,Q^2) + \tilde{\sigma}^{2\pi}(W,Q^2)$$

where

$$\tilde{\sigma}^{1\pi}(W,Q^2) = \exp\left[-\alpha(Q^2 - Q_0^2)\right] \frac{G\left(\omega'(Q^2,W); c_1, c_2, c_3\right)}{G(\omega'(Q_0^2,W); c_1, c_2, c_3)} \sigma^{1\pi}(W,Q_0^2)$$

$$\tilde{\sigma}^{2\pi}(W,Q^2) = \exp\left[-\beta(Q^2 - Q_0^2)\right] \frac{G\left(\omega'(Q^2,W); c_1', c_2', c_3'\right)}{G(\omega'(Q_0^2,W); c_1', c_2', c_3')} \sigma^{2\pi}(W,Q_0^2)$$

$Q_0^2 = 2.774\ GeV^2$ - *our anchor point.*

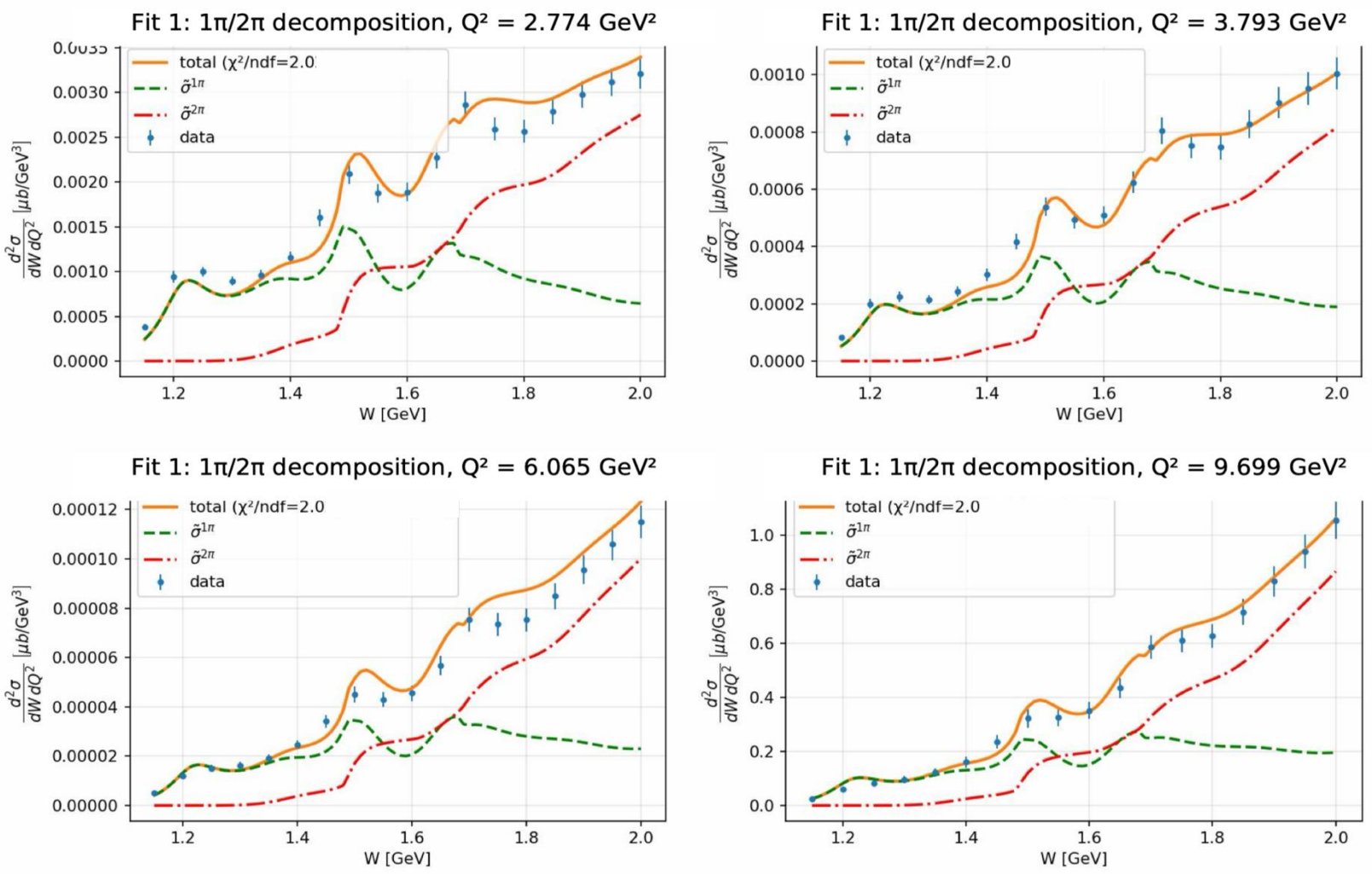
$$\omega'(Q^2,W) = 1 + \frac{W^2}{Q^2}$$

The same scaling variable used by Bloom and Gilman in the original paper

$$G(\omega'; c_1, c_2, c_3) = \sum_{i=1}^{3} c_i \left(1 - \frac{1}{\omega'}\right)^{2+i}$$

Breidenbach-Kuti polynomial

Phenomenological extension to higher Q2. “Step 3”



Fit 1 decomposition of the CLAS12 inclusive cross section

Physics of the split

- 1π (green) governs low-W and the Δ(1232).
- multimeson (red) grows with W and carries the high-W strength.
- The 1π share of the total is about 70% at the second resonance region and about 35% near W = 1.8 GeV.

Fit 2 separates longitudinal and transverse components. “Step 4”

Anchored evolution of the transverse and longitudinal pieces

$$\sigma^{\mathrm{tot.}}_{\mathrm{AO}}(Q^2, W, E_e) = c_{\mathrm{units}} \left[\tilde{\sigma}^{\mathrm{AO}}_T + \epsilon\, \tilde{\sigma}^{\mathrm{AO}}_L\right] \Gamma_{\mathrm{Hand}}\, \mathcal{J}$$

$$\tilde{\sigma}_T = \exp\left[-\alpha(Q^2 - Q_0^2)\right] \frac{G\left(\omega'(Q^2, W); c_i\right)}{G\left(\omega'(Q_0^2, W); c_i\right)} \sigma_T^{\mathrm{input}}(Q_0^2, W) \qquad \omega'(Q^2, W) = 1 + \frac{W^2}{Q^2}$$

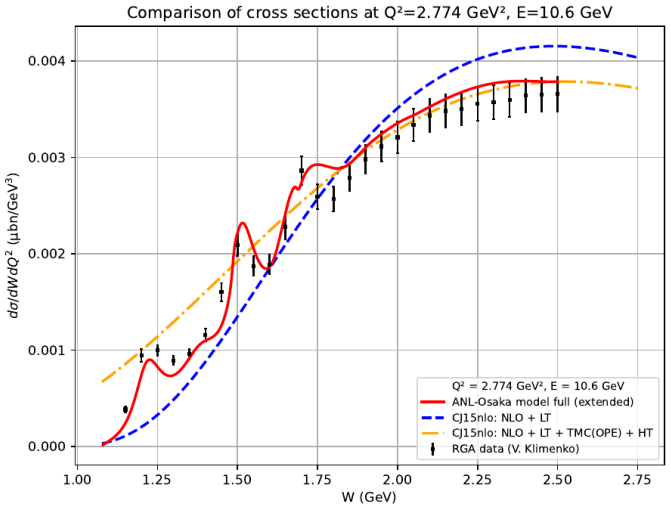
$$\tilde{\sigma}_L = \exp\left[-\beta(Q^2 - Q_0^2)\right] \frac{G\left(\omega'(Q^2, W); c'_i\right)}{G\left(\omega'(Q_0^2, W); c'_i\right)} \sigma_L^{\mathrm{input}}(Q_0^2, W)$$

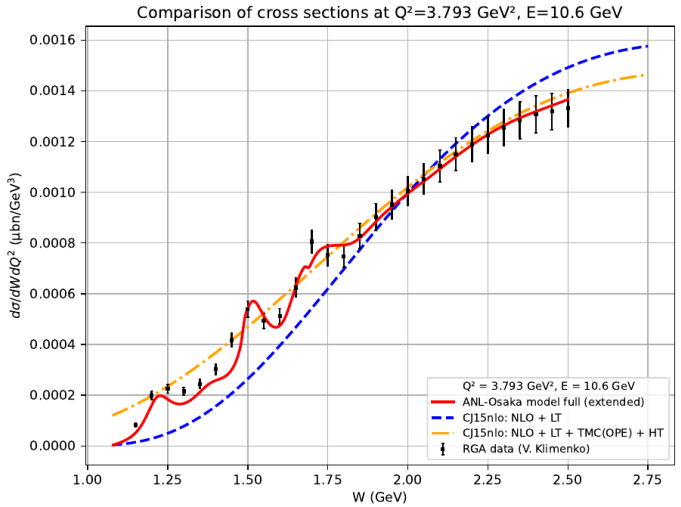
$G(\omega'; c_i)$ is a dimensionless Breidenbach–Kuti shape function, unrelated to the structure function F_2.

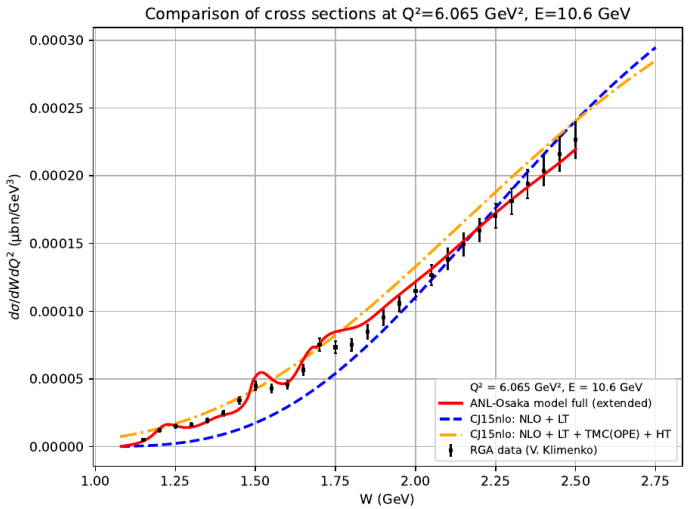
Guard-rails on the extrapolation

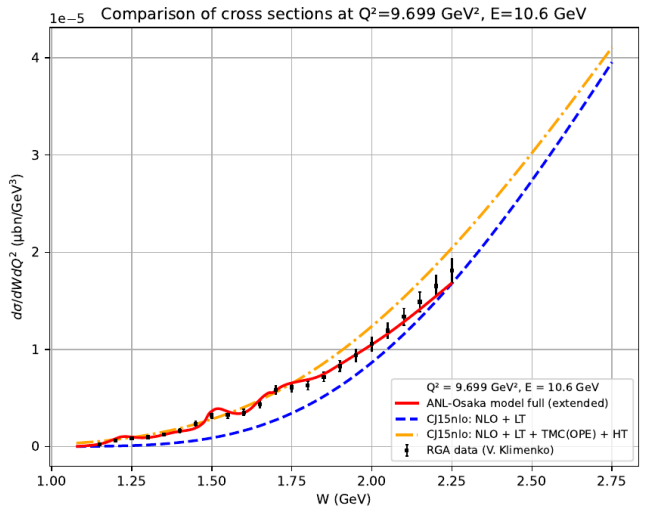
- Anchored to the data at Q_0^2 — no new resonances, no change to the underlying dynamics.
- Global minimum from a two-stage Monte Carlo search (5000 starts); uncertainties from a parametric bootstrap.
- We repeated the fit using the R_{LT} prior from CJ15 instead of ANL–Osaka. The extracted F_2 and M_2 changed very little.

Cross section comparison at higher Q^2. "Step 4"



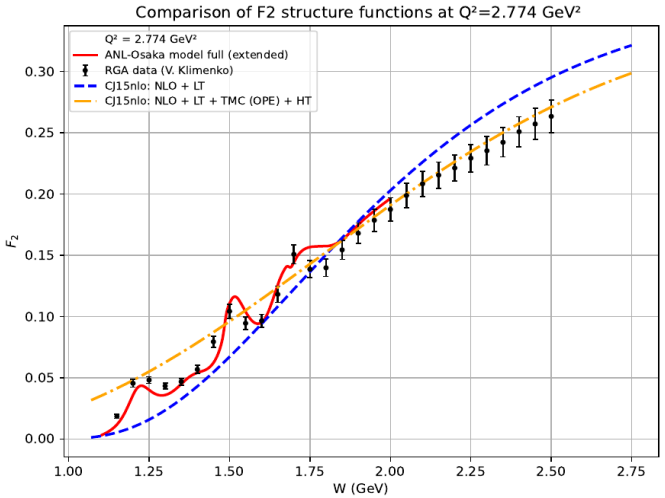


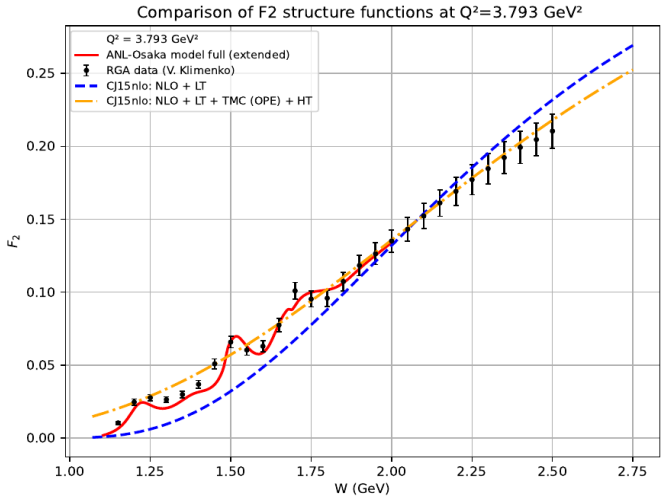


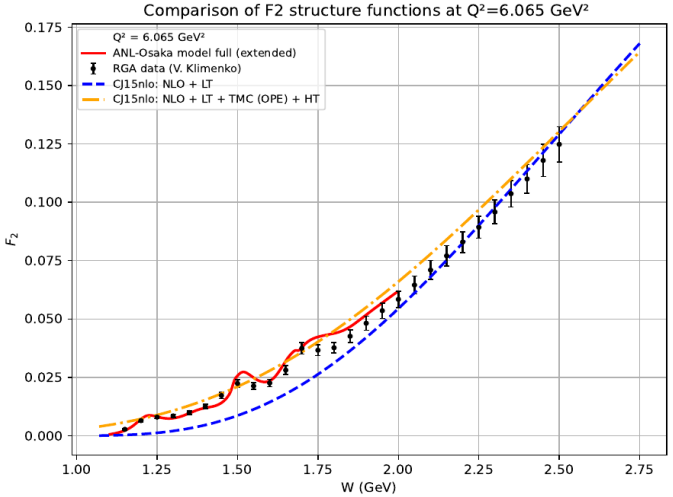


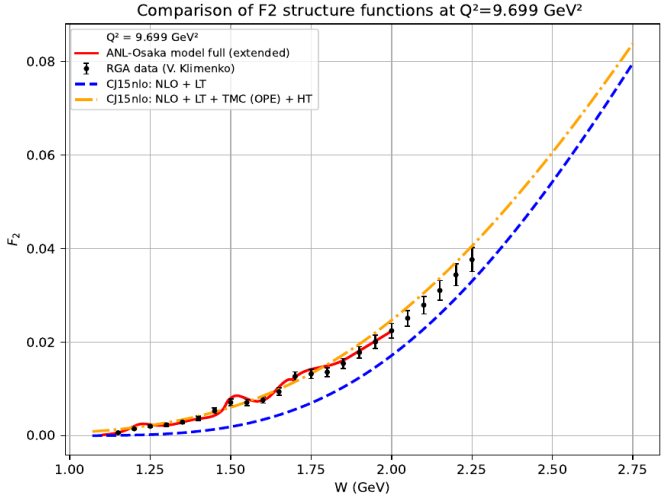
- Extended AO model curve follows the measured resonance structure
- CJ15 leading twist undershoots low W and overshoots at high W
- CJ15+TMC+HT follows the average trend above W ≈ 1.7 GeV
- The hadronic result vanishes at pion threshold by construction
- But CJ15+TMC+HT does not enforce this boundary condition

Structure function F_2 extraction and comparison. "Step 5"









- F_2 values for data (black points) are obtained within AO-constrained framework:

$$R_{LT}(W, Q^2) = \frac{\sigma_L(W, Q^2)}{\sigma_T(W, Q^2)}$$

$$F_2(W, Q^2) = C_{kinematics} \frac{1 + R_{LT}}{1 + \epsilon R_{LT}} \cdot \frac{d^2\sigma}{dW\, dQ^2}$$

- This is not a model-independent Rosenbluth separation; it is an AO-constrained extraction

- AO and data average follows CJ15NLO+TMC+HT (orange curve) – manifestation of duality

- The CJ15NLO+LT (blue curve) alone undershoots the extracted F_2 at low W, with the gap decreasing as Q^2 increases
- CJ15+LT+TMC+HT (orange) stays nonzero at the πN threshold while the extracted F_2 vanishes — a low-W distortion that later biases the 1st–2nd region moments.

Truncated moments evaluation. “Step 6”

- A quantitive test of Quark-Hadron Duality
- Isolating the contribution of individual resonance regions

$$M_2^{\mathrm{trunc}}(Q^2; W_{\mathrm{min}}, W_{\mathrm{max}}) = \int_{x(W_{\mathrm{max}})}^{x(W_{\mathrm{min}})} F_2(x, Q^2)\, dx,$$

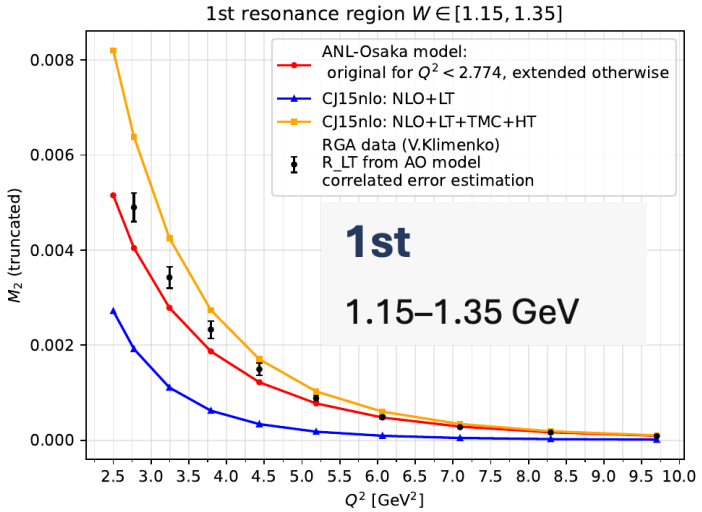
$$\text{where } x = Q^2/(W^2 - m_N^2 + Q^2)$$

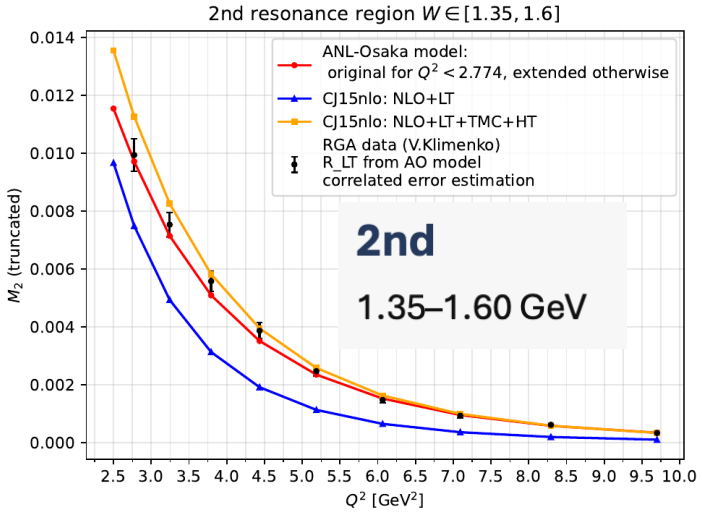
Integration ranges

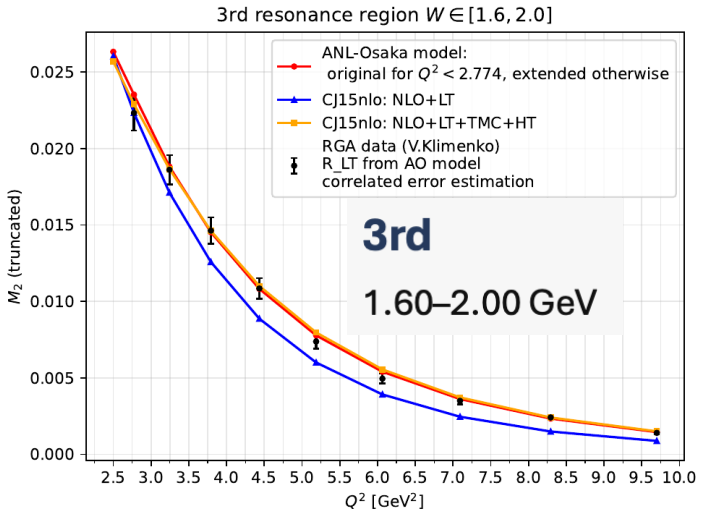
1st	2nd	3rd	High W
1.15–1.35 GeV	1.35–1.60 GeV	1.60–2.00 GeV	2.00–W_max

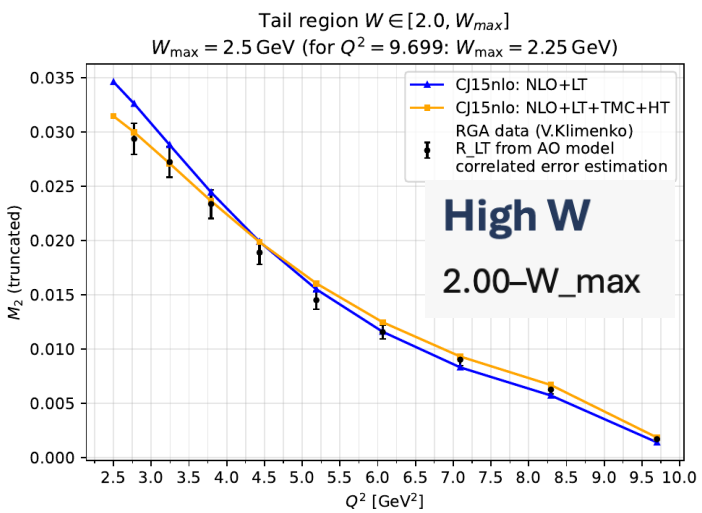
W_max = 2.5 GeV, except 2.25 GeV at Q^2 = 9.699 GeV^2

Moments: agreement except for the near-threshold region. “Step 6”





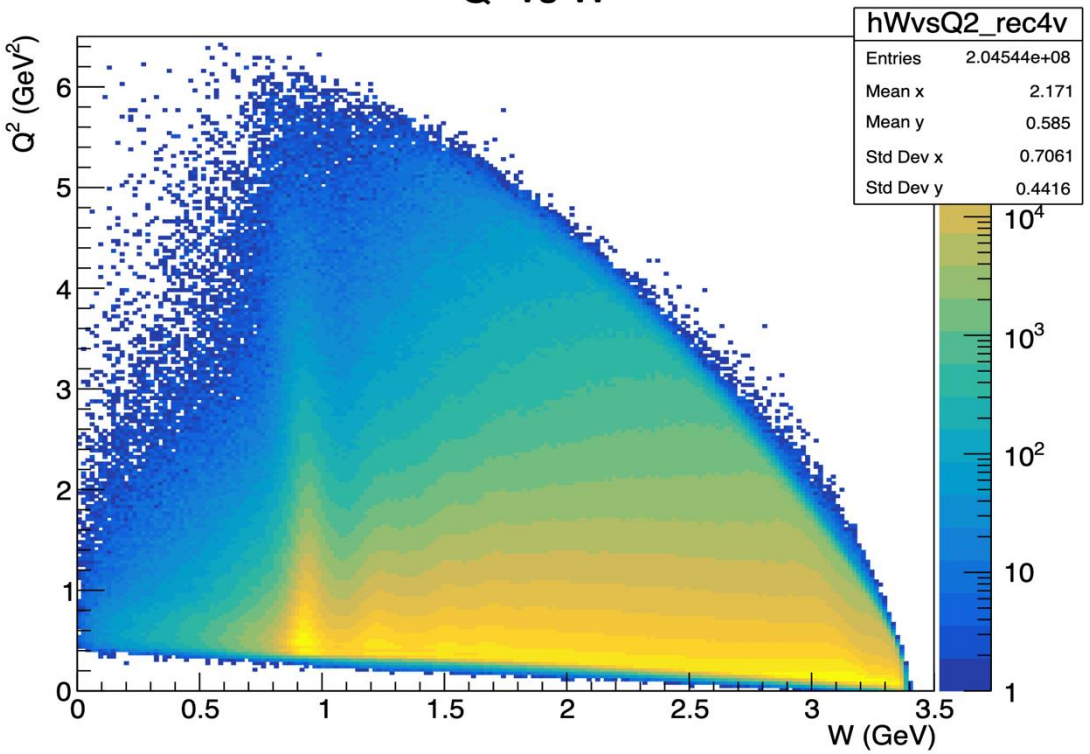




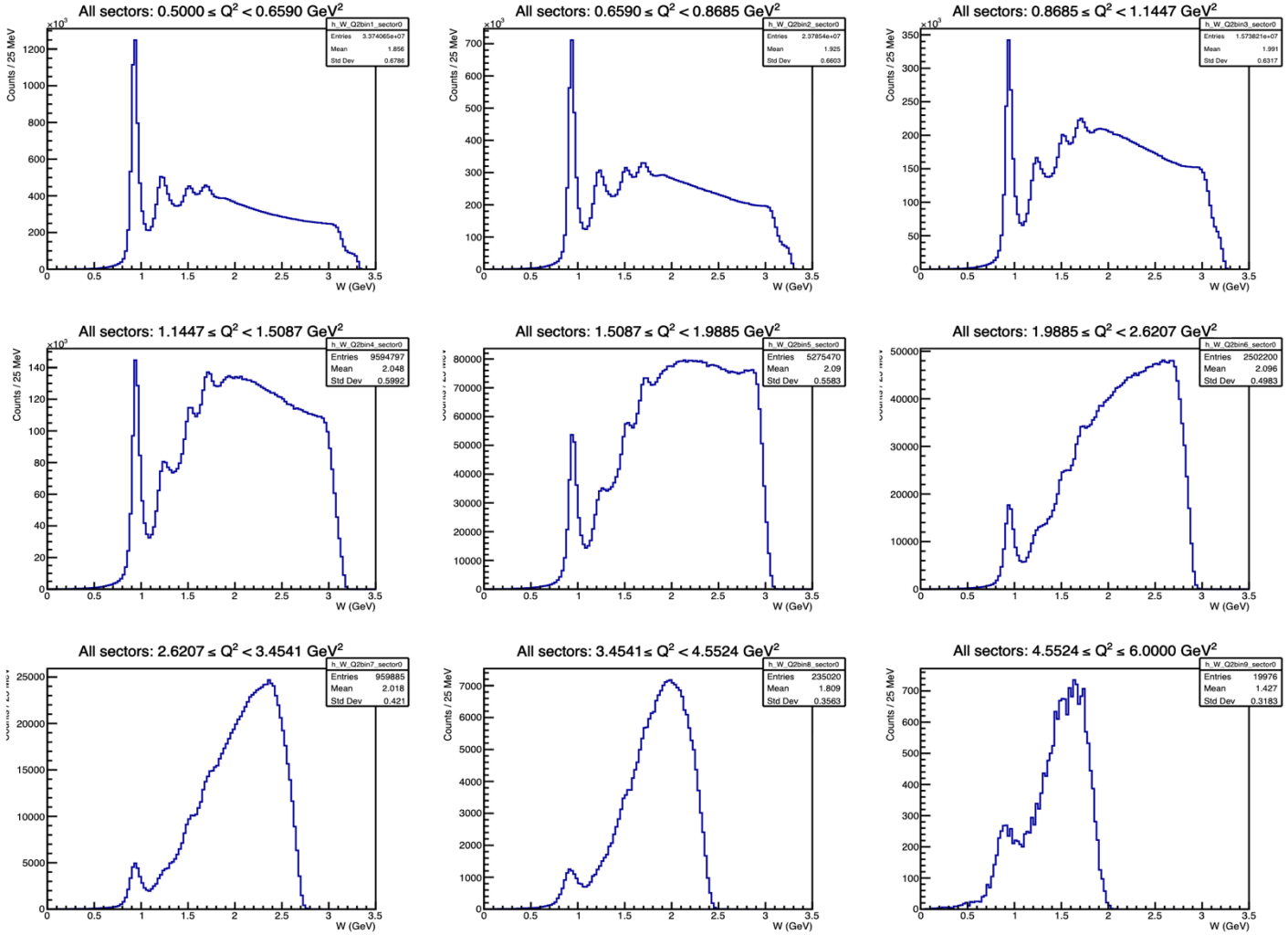
- The data is compared with the extended AO calculation (red), CJ15NLO+LT (blue), and CJ15NLO+TMC+HT (orange)
- Second, third, and high-W regions agree well with CJ15NLO+TMC+HT
- The first resonance region shows an undershoot from CJ15NLO+LT and overshoot from CJ15NLO+TMC+HT
- The discrepancy occurs in proximity to pion threshold
- **Contiguous windows ⇒ region-by-region agreement sums up to global duality**
- **Local duality ⇒ Global duality**

Ongoing RG-K inclusive analysis & duality studies @ lower Q^2

- Inclusive $e\ p \rightarrow e'\ p'\ X$ scattering
- RG-K Fall 2018 Pass 2 Outbending
- E_{beam} = 6.535 GeV
- Nine Q^2 bins: $0.5 \leq Q^2 \leq \sim 5\ GeV^2$
- W range: up to ~ 3 GeV



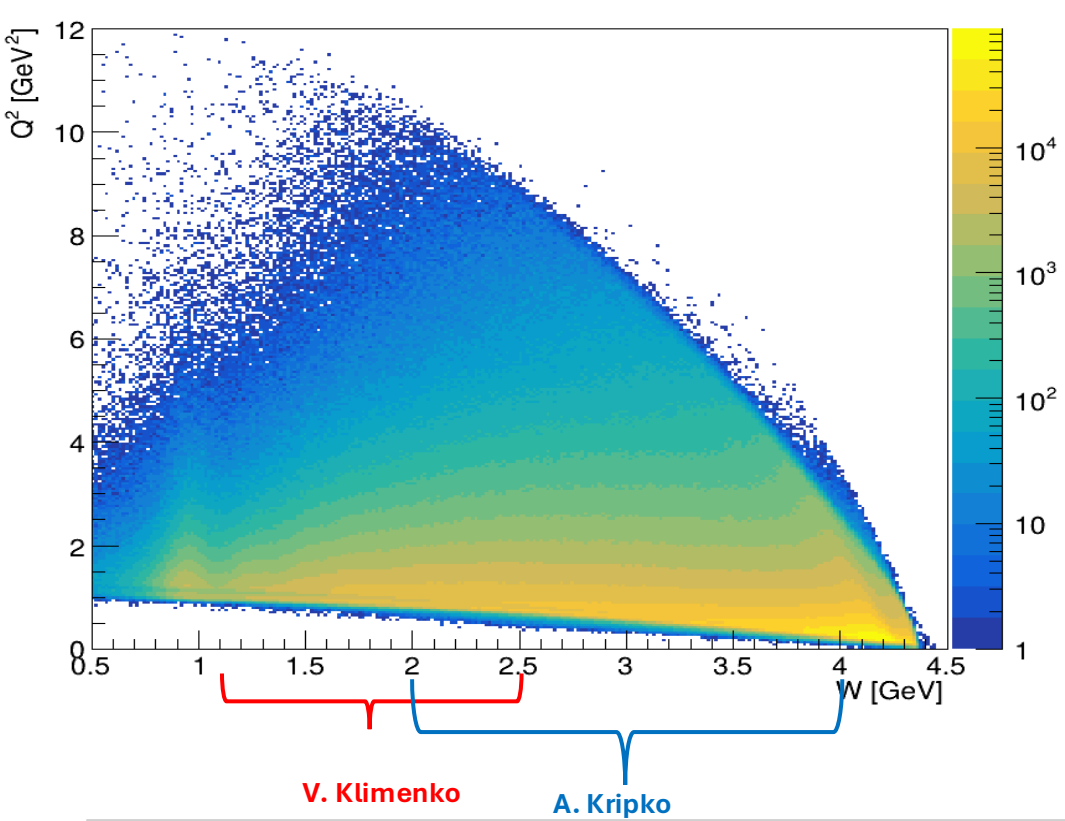
Q^2 VS W *distribution*

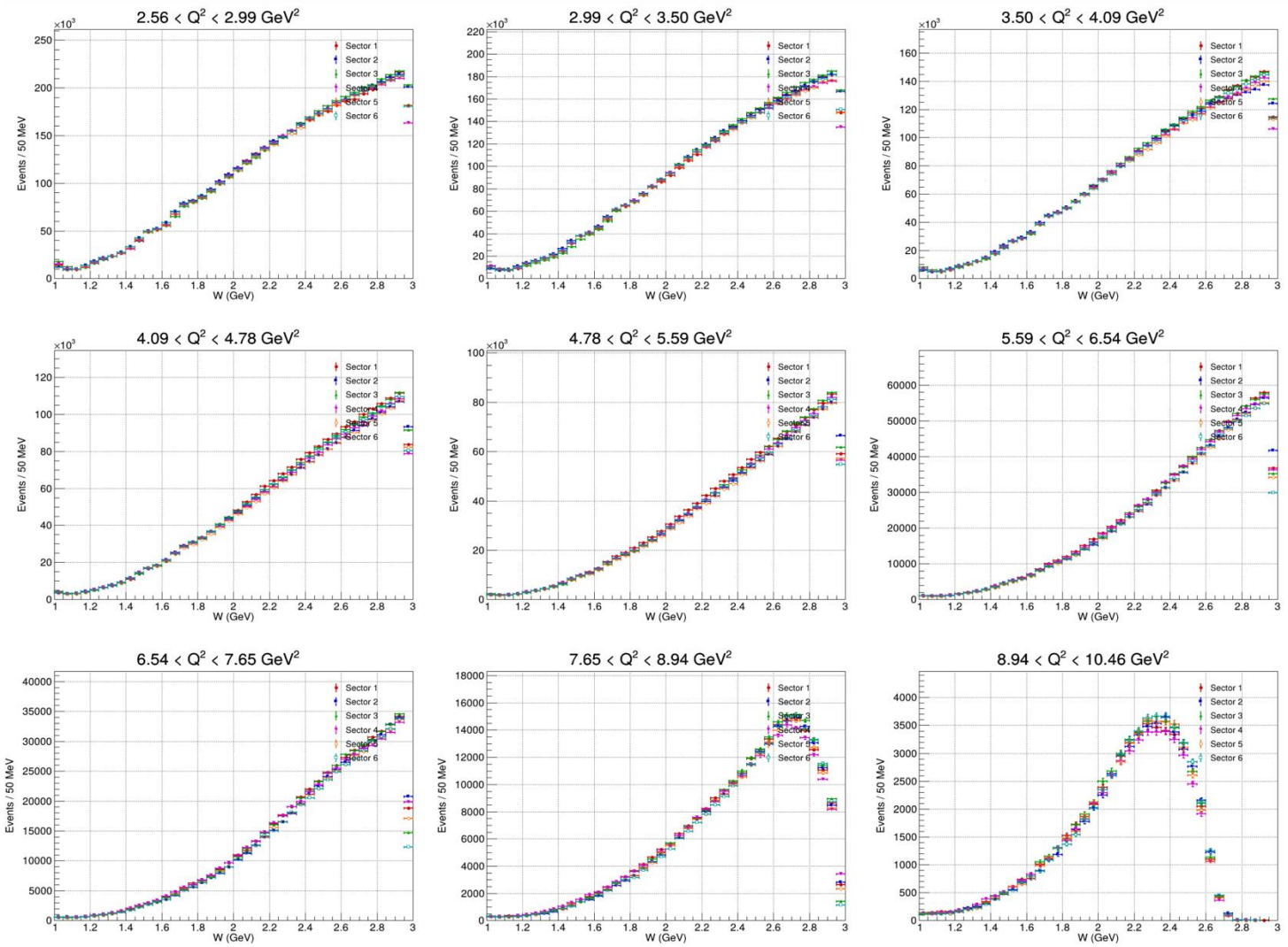


Preliminary W spectra for 9 chosen Q^2 bins

Ongoing inclusive cross section analysis in the DIS region with RG-A data

- Inclusive $e\ p \rightarrow e'\ p'\ X$ scattering
- RG-A Fall 2018 Pass 2 Inbending
- E_{beam} = 10.6 GeV
- Nine Q^2 bins: $2.55 \leq Q^2 \leq 10.4$ GeV^2
- W range: $W > 2$ GeV





Preliminary W spectra for 9 chosen Q^2 bins

Conclusions

- CLAS12 extends full resonance-region duality tests to up to $Q^2 \approx 10\ GeV^2$
- Extended ANL-Osaka describes the cross sections and enables an AO-constrained F_2 extraction
- Cross sections, F_2, and M_2 are mutually consistent with local and global duality over the measured range
- The main discrepancy is the first resonance region, which is consistent with a pion-threshold issue
- **Hadronic resonance dynamics and partonic QCD descriptions agree quantitatively when compared through averaged inclusive observables (except for the pion threshold boundary condition)**

Outlook

- Higher moments M_4 and M_6 would constrain higher-twist matrix elements directly through the OPE.
- Threshold-constrained global analyses — enforcing $F_2 \to 0$ at W_{thr} — would remove the first resonance region excess.
- Future inclusive RG-K analysis will allow to test duality at lower Q^2 around 0.5 - 5 GeV^2
- Future inclusive high W RG-A analysis will test partonic description in DIS regime
- The extracted F_2 can feed new global PDF analyses of the large-x proton.

Thank you for your attention



Backup slides

Backup: fit parameter table

TABLE I. Best-fit parameters obtained for two different R_{LT} constraints (total experimental uncertainties from the parametric bootstrap procedure). $r_i \equiv c_{i+1}/c_1$ and $r'_i \equiv c'_{i+1}/c'_1$ are the irreducible parameter combinations that fully specify the model. The $\chi^2_{\rm total}/{\rm ndf}$, $\chi^2_{\rm data}/{\rm ndf}$, and $\Phi_{\rm penalty}/{\rm ndf}$ are also quoted, with ndf $= N_{\rm data} - N_{\rm parameters}$. In the column headers, AO denotes the ANL-Osaka constraint.

Parameter	AO-constrained (adopted)	CJ15-constrained
α	-0.069 ± 0.011	-0.119 ± 0.009
β	-0.063 ± 0.011	-0.379 ± 0.030
r_1	-1.758 ± 0.499	-2.508 ± 0.252
r_2	4.495 ± 0.852	3.858 ± 0.537
r_3	-3.207 ± 0.650	-2.347 ± 0.380
r'_1	4.861 ± 0.600	-13.726 ± 0.127
r'_2	-16.958 ± 1.670	46.761 ± 1.150
r'_3	18.998 ± 1.800	-52.834 ± 2.480
$\chi^2_{\rm total}/{\rm ndf}$	2.02	2.58
$\chi^2_{\rm data}/{\rm ndf}$	2.00	1.95
$\Phi_{\rm penalty}/{\rm ndf}$	0.02	0.63

Best-fit parameters and χ^2 values for AO- and CJ15-constrained R_LT priors

The data-only χ^2/ndf remains close to 2 for both priors, so the inclusive cross sections do not strongly select either R_LT model.

From PDF-based F_1 and F_2 to the inclusive cross section

Electron kinematics at fixed W and Q^2

$$\nu = \frac{W^2 + Q^2 - M_p^2}{2M_p}, \qquad E_f = E_i - \nu, \qquad x = \frac{Q^2}{2M_p\nu}, \qquad \sin^2\frac{\theta}{2} = \frac{Q^2}{4E_iE_f}$$

Change variables from electron energy and angle to W and Q^2

$$\mathcal{J} = \frac{\pi W}{M_p E_i E_f}, \qquad \frac{d^2\sigma}{dW\,dQ^2} = \mathcal{J}\,\frac{d^2\sigma}{d\Omega\,dE_f}$$

Inclusive cross section in the one-photon exchange approximation

$$\frac{d^2\sigma}{dW\,dQ^2} = c_{\text{units}}\,\mathcal{J}\,\frac{4\alpha^2E_f^2}{Q^4}\left[2\sin^2\frac{\theta}{2}\,\frac{F_1(x,Q^2)}{M_p} + \cos^2\frac{\theta}{2}\,\frac{F_2(x,Q^2)}{\nu}\right]$$

$$c_{\text{units}} \simeq 389.38\,\mu\text{b}\,\text{GeV}^2$$

Gives $d^2\sigma/(dW\,dQ^2)$ in μb/GeV³

Higher twist contribution

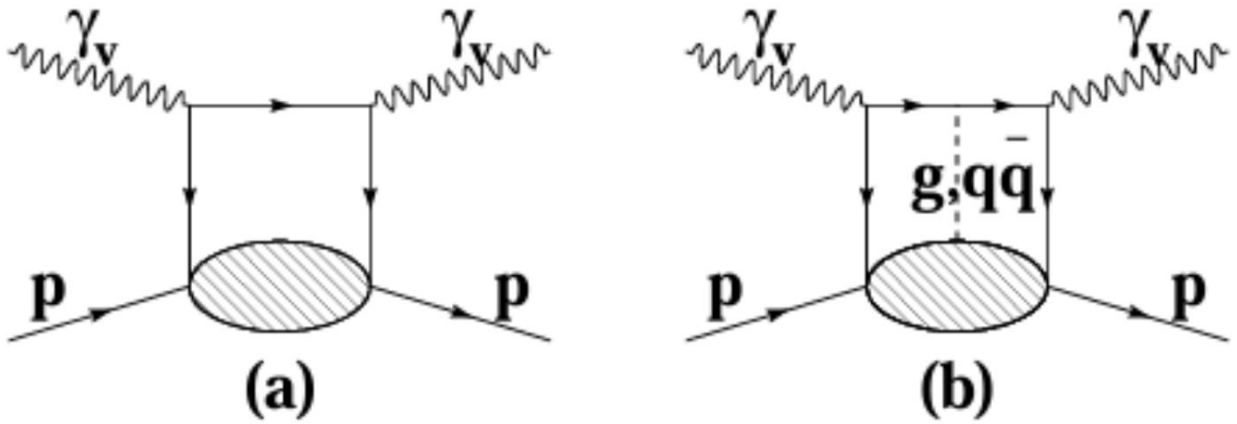


FIG. 2: Twist diagrams:(a) the leading twist contribution evaluated at leading order of pQCD; (b) the contribution of higher twists, where current quark and nucleon remnant can exchange by a system of particles consisting of gluons and $q\bar{q}$-pairs whose complexity is increasing with twist order.

Figure adapted from M. Osipenko et al., Phys. Rev. D 67, 092001 (2003).